

## STUDY ON THERMAL ANOMALIES OF EARTHQUAKE PROCESS BY USING TIDAL-FORCE AND OUTGOING-LONGWAVE-RADIATION

by

**Xuedong ZHANG<sup>a</sup>, Chunli KANG<sup>b</sup>, Weiyu MA<sup>b\*</sup>,  
Jing REN<sup>b</sup>, and Yong WANG<sup>a</sup>**

<sup>a</sup> Beijing University of Civil Engineering and Architecture, Beijing, China

<sup>b</sup> China Earthquake Networks Center, Beijing, China

Original scientific paper

<https://doi.org/10.2298/TSCI161229153Z>

*Four earthquakes above magnitude 5.0 in Yunnan and Tibet, China occurred from 2010 to 2011. By calculating the tidal-force changes induced by celestial bodies in this region, we found that the earthquakes occurred when tidal-forces continuously grew from low to peak levels and approached the maximum amplitude phase, which indicated a tidal-force that had a trigger or inducing effect of active tectonic earthquakes when the ground stress reached a critical point. At the same time analyzing the abnormal changes of outgoing longwave radiation (OLR), along with the tidal cycle, indicated that the regional distribution of the enhancement region of OLR anomalies was closely related to geologic structure, especially active faults. The OLR radiation anomaly evolved: an initial infrared rise, followed by an enhancement reaching peak, attenuation, and then a return to normal. The entire process was similar to changes observed in rock-breaking process under stress loads. Our investigation showed that the tidal-force changes caused by celestial bodies could trigger an earthquake when tectonic stress reached its critical breaking point, and the OLR anomaly was the radiation signature of the change in seismic tectonic stress. Therefore, the method of combining measurements of the tidal-force changes induced by celestial bodies with those of thermal-anomaly changes has some practical value for detecting the precursor state of impending earthquakes.*

Key words: western China, thermal infrared, tidal-force, OLR change, earthquake

### Introduction

In the 1990s, scientists studied a number of cases of strong earthquakes using the thermal infrared data of NOAA weather satellites, which showed the presence of a thermal infrared enhancement phenomenon before the earthquake [1]. Among these studies, the detection of longwave radiation anomalies near the area of the epicenter before an earthquake, using average monthly data of outgoing longwave radiation (OLR) information collected by the Earth-atmosphere system of remote-sensing satellites, has led to many valuable results in monitoring and the analysis of forecasts [2, 3]. These results obviously indicated that not only do thermal phenomena exist in the seismogenic zone, but that energy-flow whose primary characteristic is radiation also occurs. Moreover, the energy-flow spread to outer space, where it was received

\* Corresponding author, e-mail: weiyuma@163.com

by remote sensing satellites in the Earth-atmosphere system, thus comprising a new technique of using satellite remote sensing to obtain early warning of the signs of impending earthquakes [4-6].

The currently proposed methods of recognizing thermal infrared anomalies, such as image interpretation, difference analysis, heat penetrability index measurements, and point-contrast comparisons of brightness temperature anomalies, all have advantages and disadvantages. These studies showed that the differences introduced by use of normal background data has a significant impact on the research results, mainly due to the multi-year average algorithm based on the principles of statistics that eliminates the effect of heat radiation fluctuation caused by rapid, short-term changes in geologic structures. An earthquake is a quick-release process that occurs when the accumulation of tectonic stress reaches a certain intensity that exceeds the critical value of rock's elastic fracture point. Therefore, for earthquake studies, exploring the algorithms associated with seismology and mechanics is important [7]. The tidal-force induced by celestial bodies is one of the important external causes of ground stress that accumulates to reach the critical state that triggers an earthquake. The warming that occurs before an earthquake, the changes in tidal-force caused by celestial bodies, and the abnormal warming phenomenon exhibited by seismic activity, in essence, are all consistent in that they reflect the mutation of tectonic movement when tectonic movement reaches a certain degree of intensity; that is, the complementary problem becomes one of determining when short-term seismic activity occurs at the critical point to trigger an earthquake [8, 9]. The related research also shows that the tidal-force in the process of micro-earthquake is obvious, the temperature anomaly is also clearly reflected, and the tidal-force is considered to be a strong evidence of the earthquake anomaly [10]. In addition, the tidal-forces induced by celestial bodies, as the only method of pre-calculating Earth deformation phenomena at present, serves a certain indicative function in the time domain, and the degree of tectonic movement that can be measured by monitoring thermal anomalies also facilitates the discrimination of ground stress intensities [11, 12].

Yunnan and Tibet, China, were chosen as the test area in our study because the topography and geomorphology are very complex. We carried out the relevant research on the OLR abnormal radiation enhancement features of four earthquakes before the earthquakes occurred, and studied the changes of tidal-forces in these areas. This approach is well suited for testing the effectiveness of our proposed impending earthquake detection method and refining the component techniques.

### Seismogenic structure, tidal-force, and tectonic stress

In this paper, we reported on a study of four earthquakes in Yunnan and Tibet, based on measurements collected by the China Seismic Network (<http://www.ceic.ac.cn/>), the details of which are shown in tab. 1.

**Table 1. Essential characteristics of four earthquakes studied**

No.	Site	Origin time and date	Epicenter location [°]	Magnitude	Epicenter fault
1	Nierong County, Tibet	10:06, March 24, 2010	N32.4-E93.0	M5.7	Baqing-Leiniaoqi
2	Border of Dujiangyan and Pengzhou, Sichuan Province	14:11, May 25, 2010	N31.3-E103.7	M5.0	Yingxiu-Beichuan
3	Luhuo County, Sichuan Province	17:02, April 10, 2011	N31.3-E100.9	M5.3	Xianshuihe
4	Border of Tengchong and Longyang, Yunnan Province	18:16, June 20, 2011	N25.1-E98.7	M5.2	Longmenjiang

A map of the epicenter positions and active fault distributions in the earthquake regions was drawn based on the data, and is presented as fig. 1.

### Tide calculations and OLR data processing

#### Tide calculations

Solid tide refers to the cyclical elastic deformation phenomenon of the entire Earth caused by the tidal-forces of the Moon and Sun, which are considered to be the main power triggering earthquakes [13]. Solid tidal stress refers to the periodic change stress caused by solid tide in the Earth's interior [14, 15]. Much work has been done over the years on determining whether tidal stress can affect or modulate earthquakes. Wu *et al.* [16] explicitly indicated that tidal stress has a critical trigger effect for fault earthquakes in the critical stress state [17], Xi *et al.* [18] concluded that earthquakes triggered or induced by tidal-force mostly occurred near the time of the maximum value of the periodic amplitude phase [11, 19, 20], but how to judge whether the stress intensity of seismogenic tectonic movement reaches criticality was left for further study.

In our approach, we studied the relationship between origin time and the maximum value of the tidal-force's periodic amplitude phase, and analyzed the changes of OLR radiation anomalies against the background of tidal cycles using remote sensing satellite data, and further judged the change of OLR radiation anomalies whether an earthquake was triggered or not.

According to the calculation method of Calvin, the tidal generating potential  $W_i(p)$  of any point  $P$  in the Earth's interior generated by any celestial body is expressed [21]:

$$W_i(p) = g \frac{M}{r_m} \sum_{n=2}^{\infty} \left( \frac{r}{r_m} \right)^n P_n(\cos Z_m) \quad (1)$$

where  $P_n(\cos Z_m)$  is the Legendre polynomials of  $(\cos Z_m)$ ,  $Z_m$  – the zenith distance of star bodies,  $M$  – the quality of the Moon or Earth,  $g$  – the gravitational constant,  $r$  – the distance between the epicenter and geocenter,  $r_m$  – the distance between the selenocenter and geocenter, and  $r_s$  – the distance between the heliocenter and geocenter.

For the Moon, when  $n = 2$  and 3, the tidal generating potentials in the Earth's interior caused by the Moon are expressed:

$$W_{m_2}(P) = \frac{3}{4} g \frac{M_m}{r_m} \left( \frac{r}{r_m} \right)^2 \left[ \begin{aligned} & (1 - 3 \sin^2 \phi) \left( \frac{1}{3} - \sin^2 \delta_m \right) + \\ & + \sin 2\phi \sin 2\delta_m \cos H_m + \cos^2 \phi \cos^2 \delta_m \cos 2H_m \end{aligned} \right] \quad (2)$$

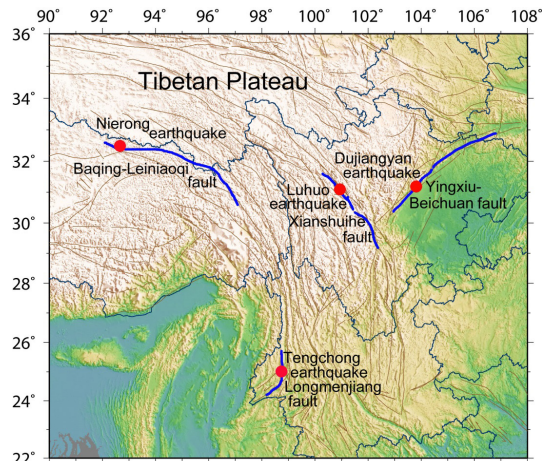


Figure 1. Map of epicenter positions and active fault distributions in the earthquake regions listed in tab. 1 (blue line denotes the seismogenic fault, red dot denotes the epicenter) (for color image see journal web site)

$$W_{m3}(P) = \frac{3}{4} g \frac{M}{r_m} \left( \frac{r}{r_m} \right)^3 \left[ \begin{aligned} & \frac{1}{3} (3 - 5 \sin^2 \phi) \sin \delta_m (3 - 5 \sin^2 \delta_m) + \\ & + \frac{1}{2} \cos \phi (1 - 5 \sin^2 \phi) \cos \delta_m (1 - 5 \sin^2 \delta_m) \cos H_m + \\ & + 5 \sin \phi \cos^2 \phi \cos 2H_m \end{aligned} \right] \quad (3)$$

Similarly, for the Sun, when  $n = 2$ , the tidal generating potential in the Earth's interior caused by the Sun is expressed:

$$W_{s2}(P) = \frac{3}{4} g \frac{M_s}{r_s} \left( \frac{r}{r_s} \right)^2 \left[ \begin{aligned} & (1 - 3 \sin^2 \phi) \left( \frac{1}{3} - \sin^2 \delta_s \right) + \\ & + \sin 2\phi \sin 2\delta_s \cos H_s + \cos^2 \phi \cos^2 \delta_s \cos 2H_s \end{aligned} \right] \quad (4)$$

For the entire Earth, then,

$$W_{\text{whole}}(P) = W_{m2}(P) + W_{m3}(P) + W_{s2}(P) \quad (5)$$

where  $\phi$  is the latitude of the epicenter,  $\delta_s$  – the declination of the Sun,  $\delta_m$  – the declination of the Moon,  $H_s$  – the zenith distance of the Sun, and  $H_m$  – the zenith distance of the Moon.

#### *The OLR data and its processing*

The OLR refers to the electromagnetic wave energy density projected by the Earth atmosphere system into outer space, measured in units of  $[\text{Wm}^{-2}]$ . Through the radiation meter aboard NOAA polar-orbit satellite, we obtain the ground longwave radiation by scanning measurements of the Earth and atmosphere in the infrared window channel (10.5-12.5  $\mu\text{m}$ ) [22-24].

The OLR data used in this study is from the global information data maintained by the U. S. National Weather Service Environmental Modeling Center (<http://www.emc.ncep.noaa.gov>), and the longwave thermal infrared radiation data has been accumulated over 30 years. Since OLR is the output result of infrared remote sensing, it is most sensitive to the sea surface and the change response to surface layer temperature. Therefore, it is considered an ideal technology for monitoring the signs of impending geologic disasters related to thermogenic phenomena [25].

In order to investigate the change features of the longwave radiation distribution field of the four studied earthquakes in Yunnan and Tibet from 2010 to 2011, the daily average grid data of the earthquakes at  $1^\circ \times 1^\circ$  were selected in their respective coverage areas (N22°-N36°, E90°-E108°) from 2010 to 2011, and the grid data constituted the value distribution field of the OLR information. Similarly, in order to extract the daily change characteristics of the OLR value distribution field of the four earthquakes before the earthquake in each region, the grid-point OLR data of an impending earthquake (day international scale) were calculated according to eq. (6) in the study area, and the value field distribution of each grid point characterizing the amount of information was obtained at the radiation enhancement area:

$$\Delta S_i(x, y) = S_i(x, y) - S_{\text{background}}(x, y) \quad (6)$$

Here  $\Delta S_i(x, y)$  is the OLR incremental value of each grid point,  $S_i(x, y)$  – the OLR value of each grid point, and  $S_{\text{background}}(x, y)$  – the OLR value of the fixed background. In this

paper, we used the lowest point of the tidal-force before the earthquake in the earthquake period as the time background, and  $x$ ,  $y$ , and  $i$  denote the latitude, longitude, and grid-point mark of the four earthquakes, respectively.

### Earthquake examples research

#### *Tidal-force change*

The tidal-force change curves with time before and after the four earthquakes were plotted using eqs. (1)-(6), and are shown in fig. 2. As can be seen from the figure, the tidal-force obviously experienced periodic change, the cycle of which is low→peak→low. All four earthquakes occurred near the maximum amplitude phase of tidal-force at the time of the earthquake, showing that they all occurred at the peak phase point of tidal-force, and also reflected a tidal-force with a triggered or induced effect for an active tectonic earthquake when ground stress reached the critical point. We need to further analyze the abnormal changes of remote sensing OLR radiation in the background of the tidal cycle in order to determine what induced the change in intensity of ground stress.

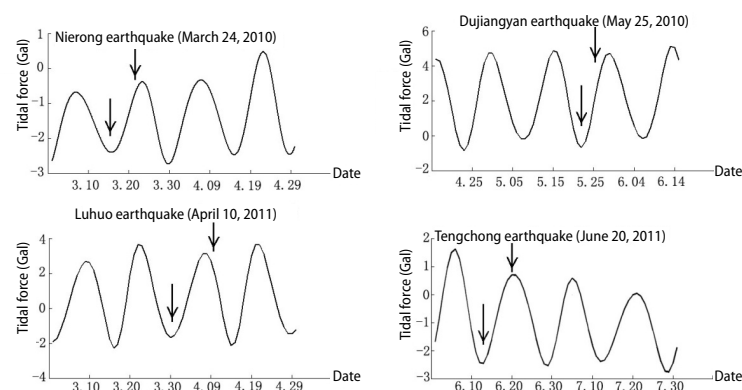


Figure 2. Sequential variation curve of tidal-force and earthquake

#### *Temporal and spatial change characteristics of OLR before an earthquake*

A large number of experiments have confirmed that the satellite infrared anomaly exhibits stage characteristics before a medium-strong earthquake. When the rock undergoes a continuous stress-state, the infrared radiation will be continually enhanced, and the infrared warming anomalies can be divided into three stages: initial warming→strengthening warming→relatively quiet. This process coincides with the process of radiation change in rock stress load-rupture [26, 27], which provides the theoretical basis of our work.

Based on the tidal cycle shown in fig. 2, the change of satellite OLR data was extracted according to eq. (6) (taking March 16 as the background of the Nierong earthquake, May 17 as that of the Dujiangyan earthquake, April 8 as that of the Luhuo earthquake, and June 13 as that of the Tengchong earthquake, and continuously subtracting, the continuous day change of OLR was obtained), as shown in figs. 3-6.

For the Nierong earthquake (fig. 3), the daily radiation field of OLR near the earthquake area showed a daily continuous increment change distribution (from March 17, 2010 to March 25, 2010). The radiation field began on March 17 (the tidal-force was at the phase point

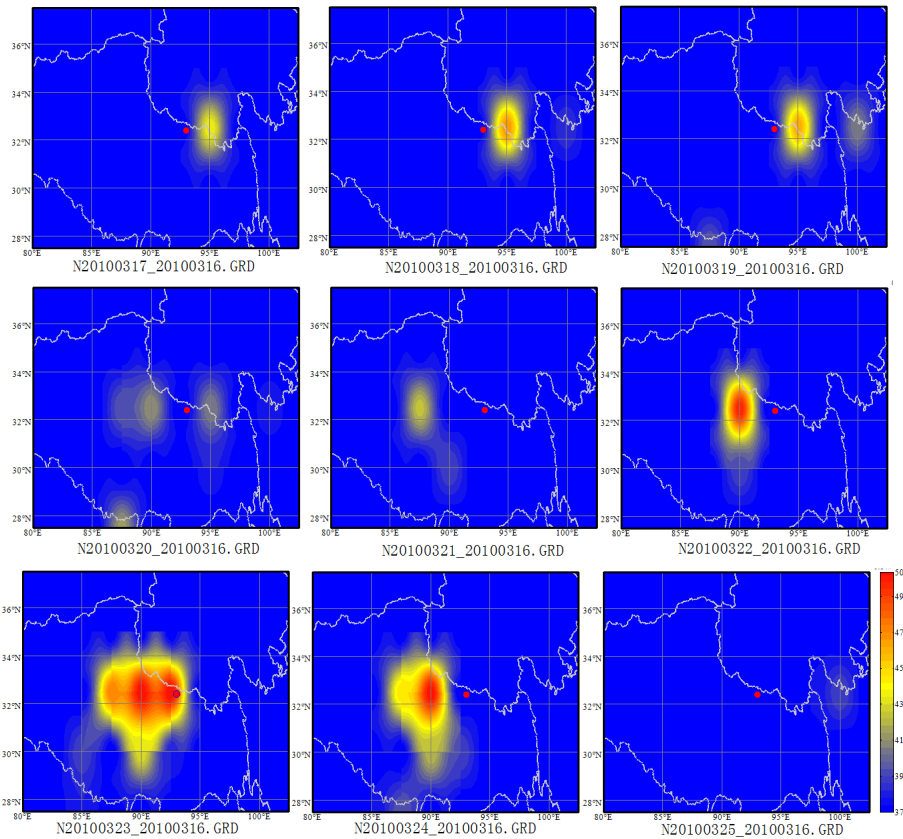


**Figure 3. Spatio-temporal evolution map of warming anomalies of the M5.7 earthquake in Nierong County, Tibet, China (red dot is the epicenter)**  
(for color image see journal web site)

near the periodic low peak), and the enhancement center of the OLR daily average incremental field moved to the west from the epicenter area, and reached its highest value on March 23, the day before the earthquake (the tidal-force was at the phase point near the periodic peak). At 10:06 on March 24 (the tidal-force was at the phase point near the periodic peak, and then decreased gradually after reaching the peak during the day), a M5.7 earthquake occurred in Nierong County. At 10:44, another earthquake, measuring M5.5 again occurred in Nierong County, after which the integrity of the terrain was destroyed. On March 25, tidal-force returned to normal conditions, and the enhancement center area of the OLR daily average radiation also completely disappeared. Combined with fig. 2, it can be seen that the radiation was constantly enhanced with the continuous enhancement of the tidal-force from low to peak, and the tectonic stress reflected by the radiation was also growing. When the tidal-force was close to peak, an earthquake occurred after the radiation reached the maximum, and the origin time was close to the maximum amplitude phase of the tidal-force.

Simultaneously, we dealt with the other three earthquakes by the same means, and the results show that they had a similar evolutionary process. That is, the earthquake occurred when the tidal-force continuously grew from low to peak levels and approached the maximum amplitude phase, and the longwave radiation experienced the following process: start-

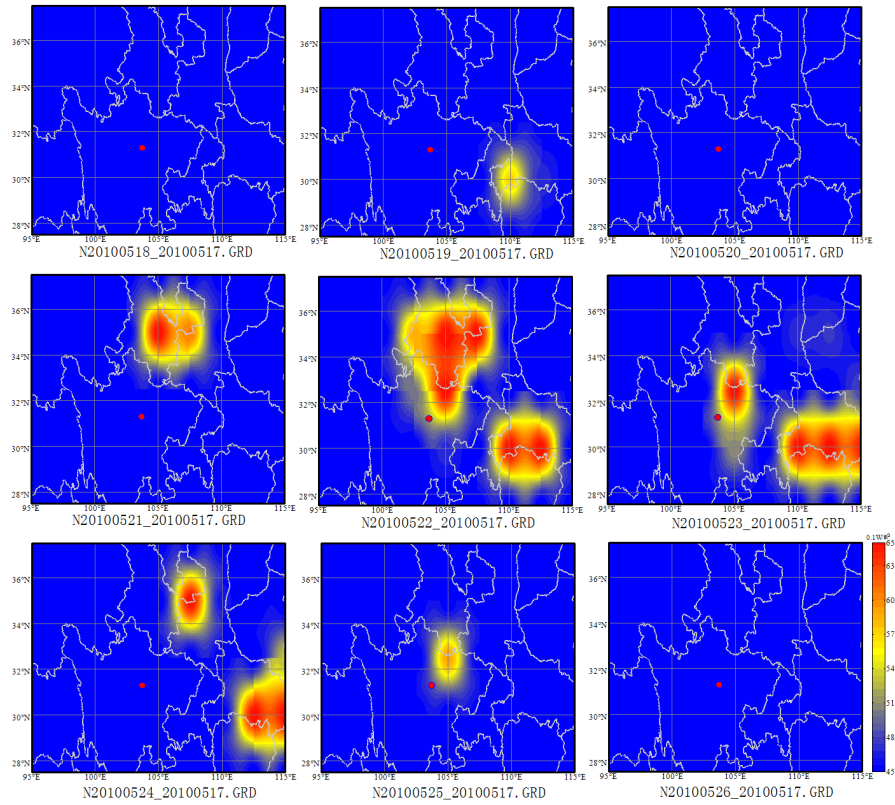


**Figure 4. Incremental field distribution of longwave radiation of the M5.0 earthquake in Dujiangyan County, Sichuan Province, China (red dot is the epicenter)**  
(for color image see journal web site)

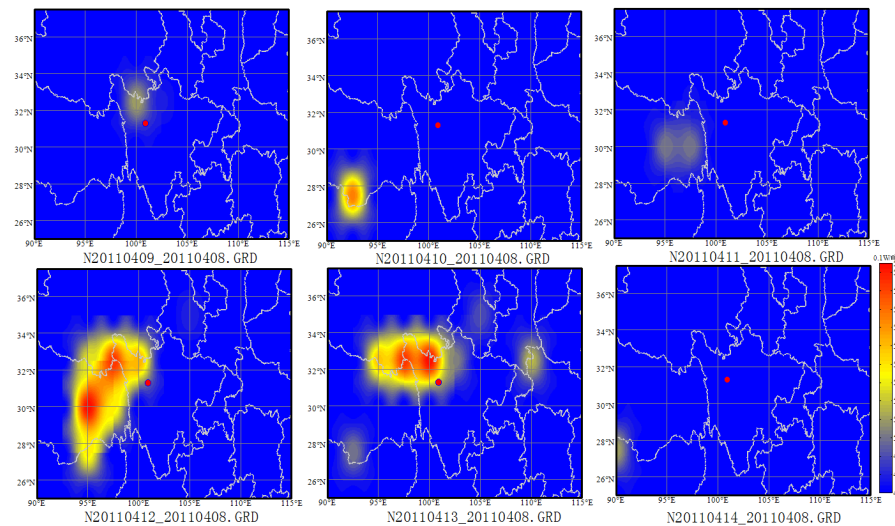


**Figure 5. Incremental field distribution of longwave radiation of the M5.3 earthquake in Luhuo County, Sichuan Province, China (red dot is the epicenter)**  
(for color image see journal web site)

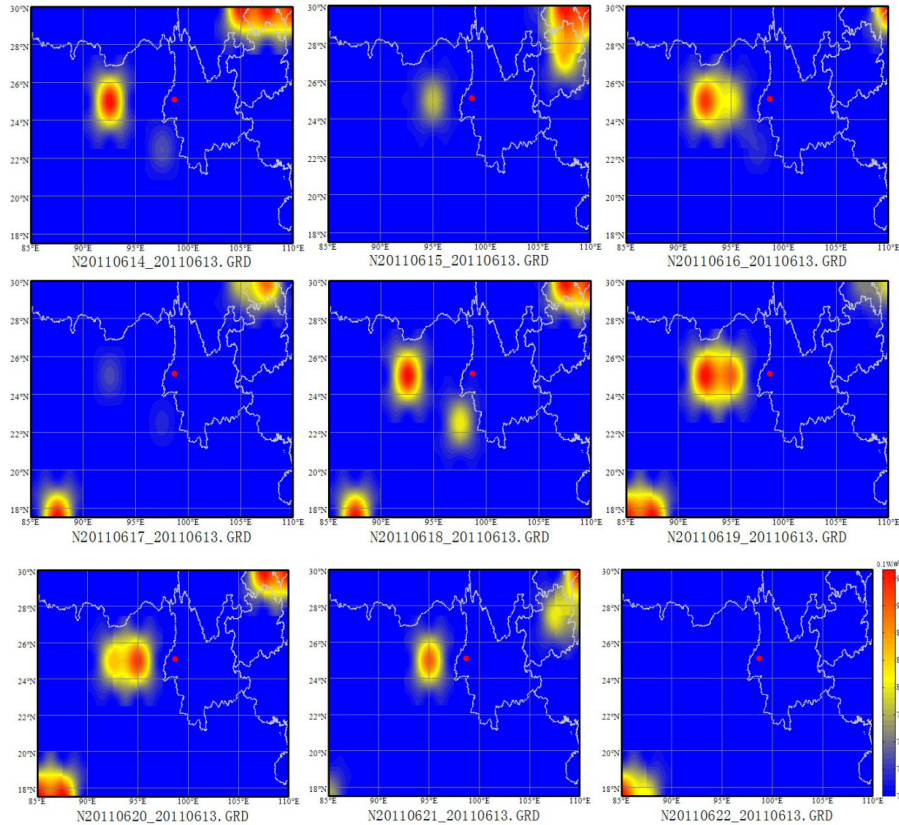


**Figure 6. Incremental field distribution of longwave radiation of the M5.2 earthquake in Tengchong County, Yunnan Province, China (red dot is the epicenter)**  
(for color image see journal web site)

ing→strengthening→peak→post-earthquake fast-fading [28]. The four earthquakes occurred upon attainment of the maximum phase point of tidal-force, which reflected tidal-force with a triggered or induced effect for an active tectonic earthquake when the ground stress reached the critical point. Through analysis of the abnormal changes of remote sensing OLR radiation in the background of the tidal cycle (figs. 3-6), and according to the regional distribution with anomalous incrementing of OLR resulting from the tidal-force and geologic structure (especially the close relation with active faults), a certain synchronism between tidal change and the increase of radiation intensity was revealed. All four earthquakes studied experienced an evolution process of increasing→peak→fast fading [29], which showed that the tidal-force had a triggering effect on the active fault when the ground stress was in a critical state.

## Discussion

Currently, due to the interference of clouds, the observation of temperature anomalies before an earthquake is frequently impeded when studying earthquake tectonic activity using remote sensing parameters. Since OLR reflects the electromagnetic energy density emitted by the Earth atmosphere system into outer space, it is the radiation quantities that most directly reflect the underlying surface properties and energy change parameters. The inversion band

(10.5-12.5  $\mu\text{m}$ ) of OLR is concentrated in the atmospheric window, which receives less interference from clouds [21]. Thus, OLR data were selected as the object of study. In the aforementioned four earthquakes studied, the images of OLR have indeed demonstrated obvious abnormal changes before an earthquake occurred, which indicates that OLR may develop into a valid data source for predicting the likely area in which an impending earthquake will occur.

Tidal-force supplemented by tectonic stress had an obvious inducing effect on an active fault whose ground stress was at the critical state (namely, the abnormal peak-recession period of OLR), but while it was the only external factor that caused the earthquake, it was not the decisive factor. The internal factor that determined the occurrence of an earthquake was the tectonic activity of the Earth's crust. The mechanism of how the change of the tidal-force modulates or induces the occurrence of an earthquake, and how it affects the abnormality of the OLR, is not still fully understood, so more earthquake cases are needed to analyze and study further. However, the existence of this kind of phenomenon, as well as the knowledge obtained in this study, indicate that the technology of using remote sensing satellites to acquire surface radiation information is viable.

## Conclusions

From the four earthquake studies previously discussed, we now have a method of obtaining an enhanced image of OLR radiation before an earthquake based on the degree of the period of tidal change. Our study reveals a continuous evolution process: pre-earthquake start→strengthening→peak→post-earthquake attenuation→calm. This process was found to be consistent with the process of radiation variation in rock stressing, loading, and rupturing. It could be concluded that the change process of pre-earthquake OLR radiation is the characterization of macroscopic radiation in the seismogenic process, which experienced the following process: appearance of initial micro-cracks of seismotectonic activities→expansion of micro-cracks→construction of large main-shock ruptures (earthquake occurrence) →affecting of all of the ruptures of active tectonics→structure adjustment→stable tightening. On the one hand, it is shown that the evolution of the critical state of ground stress can be reflected by the change of OLR radiation. On the other hand, tidal-force can change the stress-state of the structure. Furthermore, based on the effectiveness of using dynamic numerical analysis of the radiation field to extract the indications of strong earthquake anomalies on a regional scale, the method described in this paper can improve the efficiency of rapid identification of *hot* anomalies before earthquakes, and has a clear indication of the choice of background time.

## Acknowledgment

This work was jointly supported by Scientific Research Project of Beijing Educational Committee (No. SQKM201710016009 and SQKM201610016008), National Natural Science Foundation of China (No. 41401495) and Beijing Natural Science Foundation (No.8154043).

## References

- [1] Tronin, A. A., Satellite Thermal Survey – A New Tool for the Study of Seismoactive Regions, *International Journal of Remote Sensing*, 17 (1996), 8, pp. 1439-1455
- [2] Ouzounov, D., et al., Outgoing Long Wave Radiation Variability from IR Satellite Data Prior to Major Earthquakes, *Tectonophysics*, 431 (2007), 1, pp. 211-220
- [3] Pulinets, S. A., Space Technologies for Short-Term Earthquake Warning, *Advances in Space Research*, 37 (2006), 4, pp. 643-652
- [4] Kang, C. L., et al., Study of Short-Term Earthquake Prediction Indicators for Thermal Infrared Outgoing Longwave Radiation (in Chinese), *Earthquake*, 29 (2009), 1, pp. 83-89

- [5] Tronin, A. A., Thermal IR Satellite Sensor Data Application for Earthquake Research in China, *International Journal of Remote Sensing*, 21 (2000), 16, pp. 3169-3177
- [6] Bleier, T., Freund, F., Impending Earthquake Have Been Sending us Warning Signals and People Are Starting to Listen, *IEEE, Spectrum Int*, 12 (2005), pp. 17-21
- [7] Li, Y. X., et al., Relation between the Horizontal Tide Force which the Sun and Moon Imposes on the Seismogenic Zone and the Focal Mechanism (in Chinese), *Earthquake*, 21 (2001), 1, pp. 1-6
- [8] Blackett, M., et al., Exploring Land Surface Temperature Earthquake Precursors: A Focus on the Gujarat (India) Earthquake of 2001, *Geophysical Research Letters*, 38 (2011), 15, pp. 532-560
- [9] Pulnits, S. A., et al., Thermal, Atmospheric and Ionospheric Anomalies around the Time of the Colima M7.8 Earthquake of 21 January 2003, *Annales Geophysicae*, 24 (2006), 3, pp. 835-849
- [10] Chen, W. W., et al., Primary Research on the Tidal Force of Celestial Body and Temperature Change during Gaoling Ms4.4 Earthquake in Xi'an City (in Chinese), *Northwestern Seismological Journal*, 33 (2011), 1, pp. 80-83
- [11] Ma, W. Y., et al., A Preliminary Study on the Use of NCEP Temperature Images and Astro-Tidal-Triggering to Forecast Short-Impending Earthquake (in Chinese), *Seismology and Geology*, 28 (2006), 3, pp. 447-455
- [12] Heaton, T. H., Tidal Triggering of Earthquakes, *Geophysical Journal International*, 43 (1975), 2, pp. 307-326
- [13] Zhang, J., et al., A Study on Tidal Force Stress Triggering of Strong Earthquakes, *Chinese Journal of Geophysics*, 50 (2007), 2, pp. 448-454
- [14] Qin, K., et al., Quasi-Synchronous Multi-Parameter Anomalies Associated with the 2010-2011 New Zealand Earthquake Sequence, *Natural Hazards and Earth System Sciences*, 12 (2012), 4, pp. 1059-1072
- [15] Cochran, E. S., et al., Earth Tides Can Trigger Shallow Thrust Fault Earthquakes, *Science*, 306 (2004), 5699, pp. 1164-1166
- [16] Wu, X. P., et al., Tidal Stress Triggering Effects of Earthquakes Based on Various Tectonic Regions in China and Related Astronomical Characteristic, *Science China*, 52 (2009), 8, pp. 1271-1283
- [17] Bucholc, M., Steacy, S., Tidal Stress Triggering of Earthquakes in Southern California, *Geophysical Journal International*, 205 (2016), 2, pp. 681-693
- [18] Xi, Q. W., Yang, L. Z., Earth's Response to Tidal Generating Force and its Synthetic Analysis (in Chinese), *Earthquake Research in China*, 10 (1994), Suppl., pp. 83-89
- [19] Liu, J., et al., Spatio-Temporal Dynamic Variation of Thermal Anomalies before and after the 2005 Jiujiang Ms5.7 Earthquake Based on the Modulation of Additive Tectonics Stress Induced by Tide-Generating Force (in Chinese), *Acta Seismologica Sinica*, 36 (2014), 3, pp. 514-521
- [20] Miyahara, Y., et al., Correlation between Tidal Force and Occurrence of Earthquake, *Nature & Human Activities*, 21 (2010), Jan., pp. 93-108
- [21] Xi, Q. W., Hou, T. H., Earth Tides and Generating Tide Constants, *Earthquake Research in China*, 2 (1986), 2, pp. 30-41
- [22] Ma, W. Y., Abnormal Phenomenon of NCEP before Wenchuan Earthquake, *Science & Technology Review*, 26 (2008), 10, pp. 37-39
- [23] Tronin, A. A., et al., Thermal IR Satellite Data Application for Earthquake Research in Japan and China, *Journal of Geodynamics*, 33 (2002), 4, pp. 519-534
- [24] Rawat, V., et al., Anomalous Land Surface Temperature and Outgoing Long-Wave Radiation Observations Prior to Earthquakes in India and Romania, *Natural Hazards*, 59 (2011), 1, pp. 33-46
- [25] Kang, C. L., et al., The OLR Anomaly and Mechanism before Tibet Earthquake (M6.9) (in Chinese), *Progress In Geophysics*, 23 (2008), 6, pp. 1703-1708
- [26] Wu, L.X., et al., Remote Sensing-Rock Mechanics (I)-Laws of Thermal Infrared Radiation from Fracturing of Discontinuous Jointed Faults and its Meanings for Tectonic Earthquake Omens (in Chinese), *Chinese Journal of Rock Mechanics and Engineering*, 23 (2004), 1, pp. 24-30
- [27] Tramutoli, V., et al., Assessing the Potential of Thermal Infrared Satellite Surveys for Monitoring Seismically Active Areas: The Case of Kocaeli (Izmit) Earthquake, August 17, 1999, *Remote Sensing of Environment*, 96 (2005), 3, pp. 409-426
- [28] Cui, C. Y., et al., Study on the Spectral Radiative Properties of Rocks at Different Pressures (in Chinese), *Chinese Science Bulletin*, 38 (1993), 6, pp. 538-541
- [29] Liu, S. J., et al., Temporal-Spatial Evolution Features of Infrared Thermal Images Before Rock Failure (in Chinese), *Journal of Northeastern University (Natural Science)*, 30 (2009), 7, pp. 1034-1038